VNU Journal of Science: Mathematics – Physics, Vol. 38, No. 4 (2022) 100-106

VNU Journal of Science: Mathematics - Physics

Journal homepage: https://js.vnu.edu.vn/MaP

Original Article

Fabrication of SERS Substrates Based on Porous-Si Nanostructures and Silver Nanoparticles for Application in Identification of Carbendazim

Nguyen Duy Thien*, Than Thi Cuc, Vuong Van Hiep, Le Van Vu

VNU University of Science, 334 Nguyen Trai, Thanh Xuan, Hanoi, Vietnam

Received 14 July 2022
Revised 16 August 2022; Accepted 16 August 2022

Abstract: In this work, we present a quick and simple approach for fabrication of active-surface-enhanced Raman scattering (SERS) substrates based on silver nanoparticles (AgNPs) and porous silicon nanostructures (denoted by Si/Ag substrate). SERS substrates were fabricated by a 3-stage-process including the deposition of Au nanoparticles on Si wafer, etching for porous Si wafer, and coating Ag NPs on porous Si to produce SERS-active layer. To control the uniformity and cleanliness of the SERS substrate, sputtering technique was used to coat Au and AgNPs. The absorption spectra of the Si/Ag substrates exhibited a strong surface plasmon resonance absorption band of AgNPs at 425 nm. Using Si/Ag substrates to detect carbenzadim (CBZ) residue dispersed in acetone has shown that Si/Ag substrates morphology greatly affected the Raman intensity of carbendazim which opens up a promising and potential approach using SERS spectroscopy for food, environment and especially pharmaceutical applications.

Keywords: Raman, SERS, plasmon, nanoparticles, carbendazim.

1. Introduction

The using ordinary Raman spectroscopy for chemical compounds identification is restricted because of very low sensitivity of the Raman signals. Surface-enhanced Raman scattering (SERS) is a procedure which permits one to overcome this disadvantage. Starting from the observation of Fleischmann et al. [1] about SERS in 1973 for pyridine adsorbed on roughen silver surface, SERS has grown decisively, turning into an analytical tool to distinguish molecule adsorbed on metal

* Corresponding author.
E-mail address: thiennd@hus.edu.vn

https//doi.org/10.25073/2588-1124/vnumap.4765

nanostructures. By enhancing Raman signals of the analysis, SERS has opened up the chance of using Raman technique for trace chemical analysis and biomedical applications. Until now, there are two mechanisms contributing to the improvement impact of SERS. One is electromagnetic enhancement mechanism [2], the other is the chemical enhancement mechanism [3]. This intensification of SERS significantly relies upon surface morphology of SERS substrate [4], various kinds of surface morphology for SERS substrate have been reported [5], such as nanorods [6], nanowires [7], nanopillars [8], etc. In recent works, porous substrates as porous-Si [9-11], were employed for SERS applications in attempting to utilize their large surface areas and unique structures. These results indicate that porous-Si nanostructures could serve as SERS substrates with a very high sensitivity of the devices, and a good reproducibility in fabrication. SERS substrates based on porous-Si nanostructures were usually fabricated by a 3-step process: at Step 1, metal particles were deposited onto a silicon wafer (Si wafer); Step 2, Si wafer was dipped in a mixed solution of H_2O_2 and HF to create porous silicon structure, and Step 3, the porous-Si structure was again coated with the metal particles. Where, metal particles at step 1 and step 3 are usually synthesized by wet deposition procedure with $AgNO_3$ solution so it takes a long time to clean.

In this work, we report a quick and simple approach for fabrication of SERS substrates base on Ag NPs and porous Si nanostructures (referred to as Si/Ag substrate). To control the uniformity and cleanliness of the SERS substrate, sputtering technique was used to coat Au and Ag NPs. Absorption spectra of the Si/Ag substrates exhibited the surface plasmon resonance absorption band of Ag NPs centered at 425 nm. These Si/Ag substrates were used as SERS substrates to detect CBZ residue dispersed in acetone. This work showed the successfull detection of CBZ in acetone with concentrations as low as 1 ppm.

2. Experiment

First of all, sputtering technique was used to deposit an ultrathin layer of gold on Si substrates. The sputtering rate was about 12.5 nm/min. The total sputtering time was 20s to obtain the ~ 4.5 nm – thick gold layer. The substrate was then annealed at 300 ^oC in 60 min, so that the gold ultrathin film was shrank into droplets on the surface.

The next step was a wet etching to make Si substrate porous. The gold deposited Si wafer was embedded in a mixture of HF and H_2O_2 solution for 60 min. The silicon, on area without gold droplets, was moved away leaving the voids on it. The last step was to coat AgNPs on the porous-Si substrate by sputtering. By varying sputtering time one can get SERS substrates with different AgNPs layer thickness (see Figure 1).

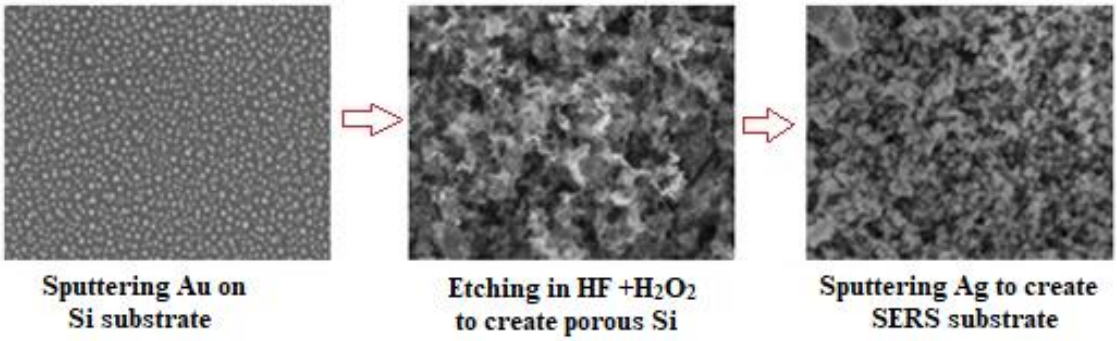

Figure 1. Si/Ag substrates fabrication schema.

The surface morphology of the samples was observed by using a field-emission scanning electron microscope (FESEM) "Nova NANOSEM 450, FEI". Crystalline structure of samples was analyzed by X-ray diffraction (XRD) using an X-ray diffractometer "SIEMENS D5005", Bruker, Germany with a scanning step of 0.03^o in 2θ diffraction angle ranging from 10 to 70^o, and with Cu-Kα1 (λ = 0.154056 nm) irradiation. Absorption spectra measurements were carried out on a VARIAN UV–VIS–NIR "Cary 5000" spectrophotometer. Raman measurements were carried out by using a LabRam "HR800", Raman spectrometer, Horiba with 632.8 nm excitation.

3. Results and Discussions

3.1. Morphology of Si/Ag Substrates

Figure 2 illustrates the morphological evolution of porous-Si and Si/Ag substrate. The results show that the pores were filled to a certain degree as the thickness of AgNPS layer on porous-Si went 5 nm up to 40 nm. Surface of Si/Ag substrate is still rough when the thickness of AgNPs layer lies in a range of 5 nm and 10 nm as in Figure 2 (Si/Ag5 and Si/Ag10). Increasing the thickness of AgNPs layer from 20 nm to 40 nm led to the disappearance of nanoporous pores on the surfaces of Si/Ag substrate. One can see that the surfaces of Si/Ag15, Si/Ag20 and Si/Ag40 are relatively smooth, indicating a full coverage of Ag on porous-Si.

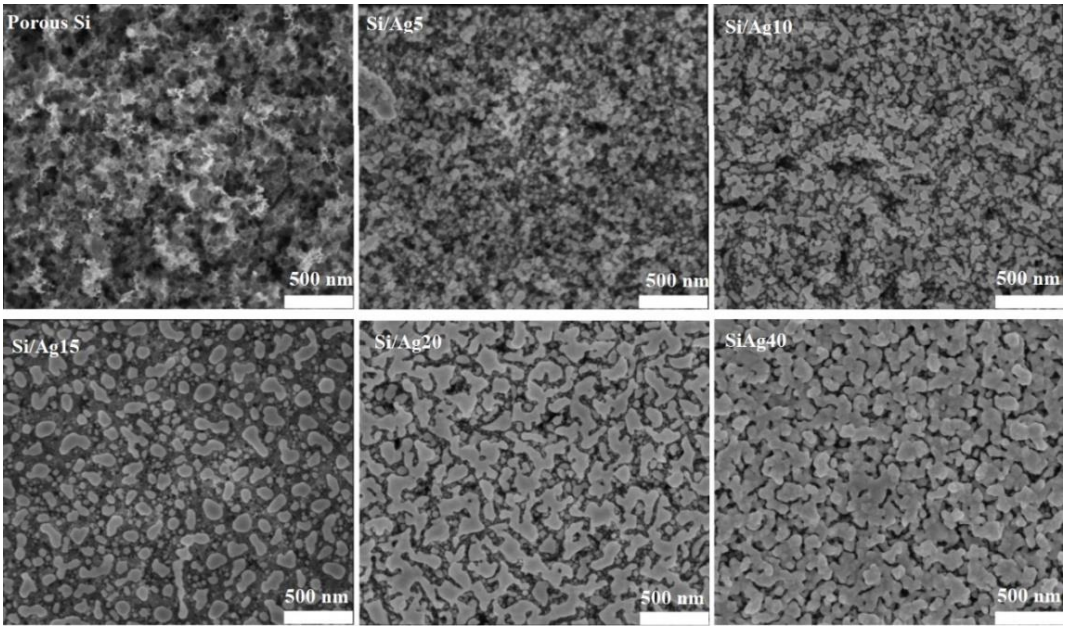

Figure 2. SEM images of porous Si and Si/Ag substrate when thickness of Ag NPS layer on porous Si went 5 nm up to 40 nm.

3.2. Structure and Absorption Spectra of Porous Si and Si/Ag Substrates

The XRD patterns of porous-Si and Si/Ag substrates are presented in Figure 3. Since Au and Ag have the same face-centered cubic (FCC) structure with almost quite similar lattice constant, it is difficult to separate their XRD peaks. However, we can see that, when the Ag NPs layer thickness increases, the diffraction peak of the samples increases greatly, indicating that the contribution of

AgNPs on the intensities of the peaks at 2θ values of 38.2˚, 44.4˚, and 64.6˚ corresponding to the diffraction planes (111), (200) and (220), respectively. The lattice constant of the FCC structure determined from the XRD pattern is of a = 4.082 Å. This is in a good agreement with the value (4.079 Å) of the standard diffraction pattern of Ag structure (CAS: 7440-57-5).

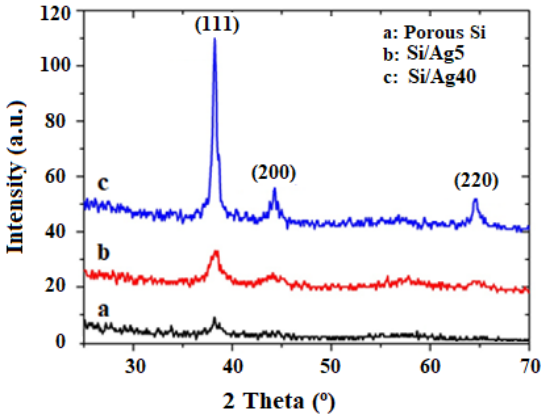

Figure 3. The XRD pattern of porous Si and Si/Ag substrate.

The average sizes of the AgNPs were estimated by Debye-Scherrer's formula [12]:

$$D = \frac{0.9\lambda}{\beta \cos\theta}$$

where β is the full width at half maximum (FWHM) in radians of the diffraction peaks, θ is the Bragg's diffraction angle and λ = 0.154056 nm. The obtained calculation gave the values of the AgNPs sizes equal to 5-7 nm. Absorption spectra of porous-Si substrate and Si/Ag substrate with AgNPs layer thickness on porous-Si of 5 nm to 40 nm obtained from the diffuse reflection data by using the Kubelka-Munk (K-M) function $F(R)$ are shown in Figure 4. The results show that AgNs layers of 5 nm, 20 and 40 nm coated porous Si substrates share similar absorption peak at 425 nm while the SERS substrate without Ag coating does not appear. The strong absorption peaks in a good agreement with surface plasmon resonance of Ag nanoparticles.

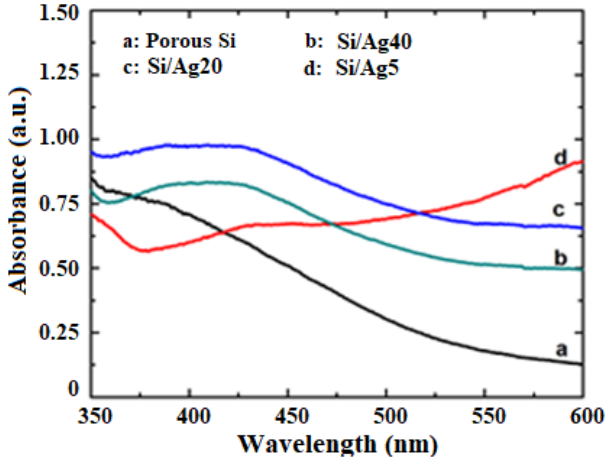

Figure 4. Absorption spectra of porous Si and Si/Ag substrate.

3.3. Si/Ag Substrates Application to Detect CBZ

The SERS spectra of CBZ (1 ppm) adsorbed on Si/Ag substrates with the thickness of AgNPs layer on porous-Si of 5, 10, 20 and 40 nm are shown in Figure 5. From these spectra one can see that Si/Ag substrates with the thickness of 20 nm and 40 nm (lines c and d) exhibit no or weak Raman peaks. Whereas, Si/Ag substrates with the layer thickness of 5 nm and 10 nm (lines a, and b) exhibit seven strong scattering peaks, at 628 cm^{-1} (C-C bending and ring stretching); 726 cm^{-1} (C-H wagging); 1,006 cm^{-1} (C-C stretch, C-N bending and C-O-CH_3 stretching); 1,222 cm^{-1} (N-H bending, C-H bending and C-C stretch), 1272 cm^{-1} (N-H bending and C-H bending), 1462 cm^{-1} (N-H bending and C-H bending) and 1,523 cm^{-1} (N-H bending and C-N stretch). This is in a good agreement with the results reported in [13].

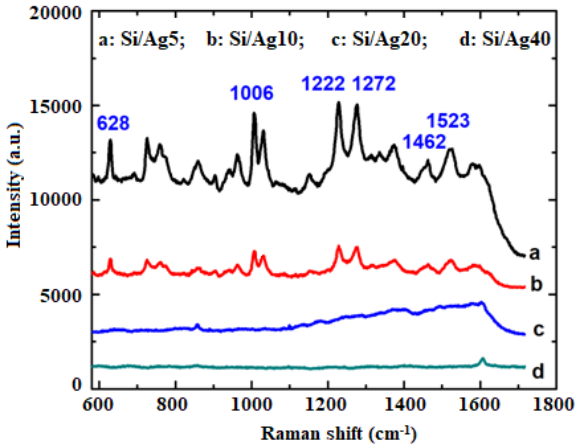

Figure 5. Raman spectrum of CBZ adsorbed on Si/Ag substrates.

According to the work of McFarland et al., [3], a Raman peak is enhanced most strongly if its wavelength satisfies equation $(\lambda_{ex} + \lambda_{vib})/2 = \lambda_{LSPS}$. In our work λ_{ex} was of 632.8 nm (He-Ne laser), $\boldsymbol{\lambda_{LSPS}}$ was of 425 nm which result in the most appropriate value of λ_{vib} for the enhancement of our SERS substrates to be of 327 nm. This value is far from CBZ Raman peaks region from 658.5 nm to 706.2 nm (data not shown), so one can conclude that the enhancement did not come from single AgNPs LSPR. The enhancement of the SERS signals can be explained by the electromagnetic mechanism. The theoretical calculations showed that the local electromagnetic field in the nano-gap region between Au or Ag nanoparticle dimers (called hot spots) is very intense due to strong electromagnetic coupling. The SERS enhancement factors in the inter-particle nano-gaps can reach up to 10^6-10^8 and depend strongly on the gap size [14-16]. In our case, both the XRD, SEM and absorption spectra indicated the presence of AgNPs on porous-Si. This suggested us about the existence of points considered as "hot spots" on our SERS substrates. Those are the nano-gaps between closely spaced interacting AgNPs where the electromagnetic field is greatly enhanced. This assumption is reinforced by comparing SEM images of AgNPs-coated porous-Si substrates (Figure 2). It can be seen that smooth surfaces provided less "hot spots" (or nano-gaps) than the rough surfaces did, the CBZ molecules may be filled in the nano-gaps between the Ag nanoparticles, leading to very high SERS enhancement factors, high measurement sensitivity and low limit of detection for CBZ.

Table 1 lists CBZ maximum residue level (CBZ MRL) for some foods recommended by Vietnam Ministry of Health. These maximum level values for CBZ are in the range from 5.0 to 20.0 ppm, they lie completely within the abovementioned limited. Thus, it is possible to develop the SERS measurement on Si/Ag substrates to quickly check the CBZ content on some foods, consequenty to

contribute to the protection of public health. However, the application problem need to be better study in further works.

Table 1. CBZ MRL for some foods recommended by Vietnam Ministry of Health

Foods	Maximum residue level [ppm]
Lettuce, mango, pineapple	5.0
Cherries	10
Rice	15
Peppers chili, dried	20

4. Conclusion

In this work the results of to the preparation of SERS substrates based on AgNPs and porous-Si nanostructures were presented. The porous-silicon structure was fabricated by MACE method with a innovation: the AuNPs and the AgNPs were coated on the substrates by sputtering, and the uniformity and cleanliness of the SERS substrate was better controlled. The influence of technological conditions on both the surface morphology of the substrates in all fabrication processes and the characteristics of Si/Ag substrate has been investigated in detail. The Si/Ag substrates exhibited a surface plasmon absorption band of AgNPs centered at 425 nm. The Si/Ag substrates were used to detect CBZ by the SERS technique, the results showed that Si/Ag substrates morphology greatly effected the Raman intensity of CBZ. The SERS spectra of CBZ showed strong scattering peaks at 628 cm^{-1}; 1,006 cm^{-1}; 1,222 cm^{-1}; 1,265 cm^{-1}; 1,462 cm^{-1} and 1,523 cm^{-1}. Using the prepared substrates for Raman analysis, the detection limit for CBZ was found to be of 1 ppm. The obtained results suggest useful application of the SERS spectroscopy in the fast determination of CBZ fungicide residue on food as well as in environments, thus contributing to the protection of public health.

References

[1] M. Fleischmann, P. J. Hendra, A. J. M. Quillan, Raman Spectra of Pyridine Adsorbed at A Silver Electrode, Chem. Phys. Lett., Vol. 26, No. 2, 1974, pp. 163-166, https://doi.org/10.1016/0009-2614(74)85388-1.

[2] S. K. Saikin, Y. Chu, D. Rappoport, K. B. Crozier, A. A. Guzik, Separation of Electromagnetic and Chemical Contributions to Surface-Enhanced Raman Spectra on Nanoengineered Plasmonic Substrates, J. Phys. Chem. Lett., Vol. 1, 2010, pp. 2740-2746, https://doi.org/10.1021/jz1008714.

[3] A. D. McFarland, M. A. Young, J. A. Dieringer, R. P. V. Duyne, Wavelength-scanned Surface-enhanced Raman Excitation Spectroscopy, J. Phys. Chem. B., Vol. 109, No. 22, 2005, pp. 11279-11285, https://doi.org/10.1021/jp050508u.

[4] K. Hering, D. Cialla, K. Ackermann, T. Dorfer, R. Moller, H. Schneidewind, R. Mattheis, W. Fritzsche, P. Rosch, J. Popp, SERS: A Versatile Tool in Chemical and Biochemical Diagnostics, Anal. Bioanal. Chem., Vol. 390, 2008, pp. 113-124, https://doi.org/10.1007/s00216-007-1667-3.

[5] D. Cialla, A. Marz, R. Bohme, F. Theil, K. Weber, M. Schmitt, J. Popp, Surface-enhanced Raman Spectroscopy (SERS): Progress and Trends, Anal. Bioanal. Chem., Vol. 403, 2012, pp. 27-54, https://doi.org/10.1007/s00216-011-5631-x.

[6] S. B. Chaney, S. Shanmukh, R. A. Dluhy, Y. P. Zhao, Aligned Silver Nanorod Arrays Produce High Sensitivity Surface-Enhanced Raman Spectroscopy Substrates, Appl. Phys. Lett., Vol. 87, 2005, pp. 031908, https://doi.org/10.1063/1.1988980.

[7] S. J. Lee, J. M. Baik, M. Moskovits, Polarization-Dependent Surface-Enhanced Raman Scattering from a Silver-Nanoparticle-Decorated Single Silver Nanowire, Nano Lett., Vol. 8, No. 10, 2008, pp. 3244-3247, https://doi.org/10.1021/nl801603j.

[8] J. D. Caldwell, O. Glembocki, F. J. Bezares, N. D. Bassim, R. W. Rendell, M. Feygelson, M. Ukaegbu, R. Kasica, L. Shirey, C. Hosten, Plasmonic Nanopillar Arrays for Large-Area, High-Enhancement Surface-Enhanced Raman Scattering Sensors, ACS Nano, Vol. 5, No. 5, 2011, pp. 4046-4055, https://doi.org/10.1021/nn200636t.

[9] S. Chan, S. Kwon, T. W. Koo, L. P. Lee, A. A. Berlin, Surface-Enhanced Raman Scattering of Small Molecules from Silver-Coated Silicon Nanopores, Adv. Mater., Vol. 15, No. 19, 2003, pp. 1595-1598, https://doi.org/10.1002/adma.200305149.

[10] A. Y. Panarin, S. N. Terekhov, K. I. Kholostov, V. P. Bondarenko, SERS-active Substrates Based on n-type Porous Silicon, Appl. Surf. Sci., Vol. 256, No. 23, 2010, pp. 6969 - 6976, https://doi.org/10.1016/j.apsusc.2010.05.008.

[11] S. M. Lok, C. S. Jin, J. B. David, P. T. Jung, A. J. Hyuk, L. S. Yup, C. Y. Kyu, A Nanoforest Structure for Practical Surface-enhanced Raman Scattering Substrates, Nanotechnology, Vol. 23, No. 9, 2012, pp. 095301, https://doi.org/10.1088/0957-4484/23/9/095301.

[12] B. E. Warren, X-ray Diffraction, Dover publications, New York, 1990.

[13] L. N. Furini, S. S. Cortes, I. L. Tocón, J. C. Otero, R. F. Aroca, C. J. L. Constantino, Detection and Quantitative Analysis of Carbendazim Herbicide on Ag Nanoparticles Via Surface-enhanced Raman Scattering, J. Raman Spectrosc., Vol. 46, No. 11, 2015, pp. 1095-1101, https://doi.org/10.1002/jrs.4737.

[14] N. D. Thien, N. N. Tu, N. Q. Hoa, S. C. Doanh, N. N. Long, L. V. Vu, Detection of Carbendazim by SERS Technique using Silver Nanoparticles Decorated SiO2 Opal Crystal Substrates. J. Electron. Mater., Vol. 48, 2019, pp. 8149-8155, https://doi.org/10.1007/s11664-019-07662-0.

[15] P. G. Etchegoin, E. C. L. Ru, A Perspective on Single Molecule SERS: Current Status and Future Challenges, Phys. Chem. Chem. Phys., Vol. 10, 2008, pp. 6079-6089, https://doi.org/10.1039/B809196J.

[16] S. Y. Ding, E. M. You, Z. Q. Tian, M. Moskovits, Electromagnetic Theories of Surface-enhanced Raman Spectroscopy, Chem. Soc. Rev., Vol. 46, No. 13, 2017, pp. 4042-4076, https://doi.org/10.1039/C7CS00238F.